ehp ENVIRONMENTAL HEALTH PERSPECTIVES
http://www.ehponline.org

Effects of Tributyltin Chloride on Cybrids with or without an ATP Synthase Pathologic Mutation

Ester López-Gallardo, Laura Llobet, Sonia Emperador, Julio Montoya, and Eduardo Ruiz-Pesini

http://dx.doi.org/10.1289/EHP182

Received: 1 September 2015
Revised: 27 November 2015
Accepted: 13 April 2016
Published: 29 April 2016

Environ Health Perspect DOI: 10.1289/EHP182
Advance Publication: Not Copyedited

Effects of Tributyltin Chloride on Cybrids with or without an ATP Synthase Pathologic Mutation

Ester López-Gallardo[1,2,3], Laura Llobet[1,2,3], Sonia Emperador[1,2,3], Julio Montoya[1,2,3], and Eduardo Ruiz-Pesini[1,2,3,4]

[1]Departamento de Bioquímica, Biología Molecular y Celular; [2]Instituto de Investigación Sanitaria de Aragón; [3]CIBER de Enfermedades Raras (CIBERER); [4]Fundación ARAID. Universidad de Zaragoza, Zaragoza, Spain

Address correspondence to Eduardo Ruiz-Pesini (eduruiz@unizar.es) and Julio Montoya (jmontoya@unizar.es), Departamento de Bioquímica, Biología Molecular y Celular, Universidad de Zaragoza. C/ Miguel Servet, 177. 50013-Zaragoza, Spain. Telephone: +34-976761640. Fax: +34-976761612.

Short running title: Xenobiotic mitochondriopathies

Acknowledgments: We would like to thank Santiago Morales for his assistance with the figures. This work was supported by grants from the Instituto de Salud Carlos III (FIS-PI14/00005 and PI14/00070); Departamento de Ciencia, Tecnología y Universidad del Gobierno de Aragón (Grupos Consolidados B33) and FEDER Funding Program from the European Union; and Fundación ARAID-Programa de Apoyo a la I+D+I para jóvenes investigadores 2010. L.L. has a fellowship from Instituto de Salud Carlos III [FI12/00217]. CIBERER is an initiative of the ISCIII.

Competing financial interests: The authors declare they have no actual or potential competing financial interests.

ABSTRACT

Background: The oxidative phosphorylation system (OXPHOS) includes nuclear chromosome (nDNA)- and mitochondrial DNA (mtDNA)-encoded polypeptides. Many rare OXPHOS disorders, such as striatal necrosis syndromes, are due to genetic mutations. Despite important advances in sequencing procedures, causative mutations remain undetected in some patients. It is possible that etiologic factors, such as environmental toxins, are the cause of these cases. Indeed, the inhibition of a particular enzyme by a poison could imitate the biochemical effects of pathological mutations in that enzyme. Moreover, environmental factors can modify the penetrance or expressivity of pathological mutations.

Objectives: To study the interaction between p.MT-ATP6 and an environmental exposure that may contribute phenotypic differences between healthy individuals and patients suffering from striatal necrosis syndromes or other mitochondriopathies.

Methods: We analyzed the effects of the ATP synthase inhibitor tributyltin chloride (TBTC), a widely distributed environmental factor that contaminates human food and water, on transmitochondrial cell lines with or without an ATP synthase mutation that causes striatal necrosis syndrome. Doses were selected based on TBTC concentrations previously reported in human whole blood samples.

Results: TBTC modifies the phenotypic effects caused by a pathological mtDNA mutation. Interestingly, wild-type cells treated with this xenobiotic show similar bioenergetics when compared with the untreated mutated cells.

Conclusions: In addition to the known genetic causes, our findings suggest that environmental exposure to TBTC might contribute to the etiology of striatal necrosis syndromes.

INTRODUCTION

The mitochondrial DNA (mtDNA) m.8993T>G transversion in the *MT-ATP6* gene provokes a p.L156R substitution in the transmembrane helix 4 (TMH4) of the p.MT-ATP6 subunit. This polypeptide is an ATP synthase (complex V, CV) component of the oxidative phosphorylation system (OXPHOS). The amino acid position 156 is located in the channel used by protons to enter the mitochondrial matrix and power the ATP synthesis. The m.8993T>G mutation is associated with maternally inherited Leigh syndrome (MILS) and neurogenic muscle weakness, ataxia and retinitis pigmentosa (NARP) (Holt et al. 1990; Thorburn and Rahman 1993). As a generalization, NARP is caused by moderate levels of the m.8993T>G mutation, whereas individuals with mutant loads greater than 90 % have MILS (Tatuch et al. 1992). However, in some families, oligosymptomatic children share the same mutation load of symptomatic siblings (Enns et al. 2006), and high mutation loads are not always associated with MILS or NARP signs (Degoul et al. 1995; Mkaouar-Rebai et al. 2009; Tsao et al. 2001). Similar to many other pathological mutations (Cooper et al. 2013; Lake et al. 2015), other factors are likely involved in the phenotypic differences among individuals with the same m.8993T>G mutation load.

Other pathological mutations in mtDNA genes have been reported in MILS patients (Montoya et al. 2009; Ruhoy and Saneto 2014; Thorburn and Rahman 1993). Thus, polymorphic variation in these genes may influence the m.8993T>G phenotype. Indeed, the mtDNA genetic background (mtDNA haplogroups) plays an important role in modulating the biochemical defects and clinical outcome by altering the risk of MILS due to m.8993T>G (D'Aurelio et al. 2010; Hao et al. 2013). Moreover, many other pathological mutations in nuclear DNA (nDNA) genes have

been described in Leigh syndrome (LS) patients (Ruhoy and Saneto 2014). For example, a mutated mitochondrial aminoacyl-tRNA synthetase was described in a LS patient (Schwartzentruber et al. 2014). Interestingly, a MILS patient had a homoplasmic mutation in the $tRNA^{Val}$ and his clinically normal mother was also homoplasmic mutant (McFarland et al. 2002). It was recently shown that the overexpression of the mitochondrial valyl-tRNA synthetase can restore the steady-state levels of the mutated $tRNA^{Val}$. Thus, inter-individual variations of this synthetase may underlie clinical differences (Rorbach et al. 2008). Therefore, polymorphic variation in nDNA genes may influence the m.8993T>G phenotype.

In addition to nuclear and mitochondrial genetic factors, environmental stimuli may modify the phenotype of the m.8993T>G mutation. Certain chemicals trigger the appearance of pathological phenotypes associated with mtDNA mutations. For example, individuals harboring the m.1555A>G transition in the *MT-RNR1* gene for the 12S rRNA suffer non-syndromic hearing loss when exposed to aminoglycosides (Prezant et al. 1993). Furthermore, occupational exposure to n-hexane and other solvents precipitated visual failure in a Leber hereditary optic neuropathy patient with the m.11778G>A mutation (Carelli et al. 2007). Previous reports suggest that the CV proton channel, particularly the p.MT-ATP6 subunit, is the target site for organotin compounds, including tributyltin chloride (TBTC) (von Ballmoos et al. 2004). These compounds contaminate human food and water (Kotake 2012). Therefore, it is possible that TBTC affects the expressivity of the m.8993T>G mutation.

MATERIALS AND METHODS

Transmitochondrial cell line construction, characterization and functional investigations

To homogenize nuclear and environmental factors, we built transmitochondrial cell lines (cytoplasmic hybrids or cybrids) with osteosarcoma 143B or adenocarcinoma A549 rho^0 nuclear backgrounds using patient and control platelets (Chomyn et al. 1994). All samples were collected with informed consent, and the Ethics Review Committees of the involved hospitals and the Government of Aragón approved the study (CEICA 11/2010).

The cybrids were grown in Dulbecco's modified eagle medium containing glucose (1 g/l), pyruvate (0.11 g/l) and fetal bovine serum (5 %) with no antibiotics (Llobet et al. 2015a).

For molecular cytogenetic analysis, cells were exposed to colchicine (0.5 µg/ml) for 4 h at 37 °C and harvested routinely. Metaphases were prepared following a conventional cytogenetic protocol for methanol: acetic acid (3:1)-fixed cells. Approximately 20 metaphase cells were captured and analyzed for each cell line. The genetic fingerprint of the cybrid cell lines was determined using an AmpFLSTR® Identifiler® PCR Amplification Kit (Life Technologies) and an ABI Prism 3730xl DNA analyzer (Applied Biosystems). These genetic fingerprints were compared with those from the American Type Culture Collection (ATCC) cell lines. To confirm the nucleotide at the m.8993 position, a PCR-RFLP analysis was performed (Lopez-Gallardo et al. 2014). The mtDNA sequences were obtained using a BigDye Terminator v 3.1 Cycle Sequencing Kit (Applera Rockville) and an ABI Prism 3730xl DNA analyzer. The revised Cambridge reference sequence (GenBank NC_012920) and an mtDNA phylogenetic tree were used to locate mutations and define mtDNA haplogroups (van Oven and Kayser 2009),

respectively. The level of peroxisome proliferator-activated receptor gamma (PPARγ) mRNA was determined in triplicate using RT-qPCR and the One-Step Real-Time system (Applied Biosytems). The expression levels were normalized using 18S rRNA. The ΔCt method was used to calculate fold expression. StepOne software version 2.0 (Applied Biosystems) was used for data analysis.

The analyses of oxygen consumption, ATP and H_2O_2 levels were performed in triplicate according to previously described protocols (Gomez-Duran et al. 2010). The determination of the mitochondrial inner membrane potential (MIMP) was performed using a Mito-ID Membrane Potential Detection Kit (Enzo Life Sciences). Fluorescent microscopy was performed on live cells using a Floyd Cell imaging station (Life Technologies). Isocitrate dehydrogenase (IDH) activity was determined using a commercial Isocitrate Dehydrogenase Colorimetric Assay Kit (Abcam®), according to the manufacturer's instructions. Briefly, 1 x 10^6 cells grown in DMEM were lysed in 200 µl of an assay buffer provided in the kit. The lysate was centrifuged at 13,000 x g for 10 min, and the cleared supernatant was used for the assay. NAD^+ was used as the substrate for the NAD-IDH assay. The measurements were obtained using a NovoStar MBG Labtech microplate instrument.

In a previous study, 25 out of 32 blood donors from Michigan, USA, showed TBT detectable concentrations in whole blood samples (Kannan et al. 1999). The observed range, 8.3 - 293 nM, encompasses TBTC concentrations used in this study. When required, TBTC (Sigma-Aldrich) or oligomycin (OLI) (Sigma-Aldrich), another CV inhibitor, were solved in ethanol and added to the respiration medium during the oxygen consumption determination and to the medium for ATP, MIMP, H_2O_2 or IDH determination during the 2 h, 15 min, 30 min and 24 h of incubation, respectively.

Statistical analysis

The statistical package StatView 6.0 was used to perform all statistical analyses. The data are presented as the mean and standard deviation. At least three analyses were performed for each parameter. An unpaired two-tailed t-test was used to compare parameters. Linear regression analyses were performed and linear regression equations and regression coefficients are indicated for TBTC concentrations vs. oxygen consumption, ATP amount, or H_2O_2 levels. P values < 0.05 were considered statistically significant.

RESULTS

Characterization of the cybrid cell lines

Five cybrid cell lines were built. Two cybrids within the adenocarcinoma A549 nuclear background should harbor the m.8993T (Awt) or m.8993G (Am) mtDNA alleles. The other three cybrids within the osteosarcoma 143B nuclear background should also harbor the m.8993G (Om) or m.8993T mtDNA alleles. For the osteosarcoma 143B m.8993T cells, a non-isogenic wild-type cybrid was first generated (Owt). An isogenic cybrid was produced (Owti) after we obtained platelets from the wild-type mother of the mutant patient.

Karyotyping was used to verify that the nuclear backgrounds were equivalent. Thus, the Am and Awt cybrids share the modal number of chromosomes (60) and several chromosomal abnormalities [del(2p21), +der(6)t(1;6)(q24-25?;q23), +der(7)delq32?, del(11q23)] (see

Supplemental Material, Figure S1). The modal number of chromosomes differs in Owt (66), Owti (69), and Om (70/71) cybrids,; however, these numbers are similar to those previously published in other osteosarcoma 143B transmitochondrial cell lines (Gomez-Duran et al. 2010). These cybrids share several chromosomal abnormalities [+i(7p), +der(7)t(1;7)(q25;q32)[2], +der(12)add(q24.3)]. To confirm the cell origin of our cybrids and the equivalence of nuclear backgrounds, we determined the nuclear genetic fingerprint of 16 short tandem repeats (STRs) (see Supplemental Material, Table S1). Adenocarcinoma A549 cybrids do not differ in STR markers and do not vary from the 9 STR markers characterized for the ATCC adenocarcinoma A549 cell line. The same is true for the osteosarcoma 143B cybrids and the ATCC osteosarcoma 143B cell line.

Next, we confirmed the mtDNA alleles of the cybrids using PCR-RFLP. The m.8993T>G mutation caused the amplicon to be cut in two fragments, and the wild-type amplicon was not digested (see Supplemental Material, Figure S2). To rule out the presence of mtDNA non-defining haplogroup (private) mutations that can affect the bioenergetic phenotypes of these cybrids, we sequenced the complete mtDNA (GenBank JN635299, KJ742713, KJ742715, KT002148, KT002149) (see Supplemental Material, Figure S2). Owt cybrids contained two non-synonymous private mutations: m.3387T>A provoking a p.MT-ND1:I27M substitution and m.14189A>G causing a p.MT-ND6:V162A change. Am cybrids contained one non-synonymous private mutation: m.9194A>G producing a p.MT-ATP6:H223R replacement. These mutations have been previously found 0, 9 and 4 times, respectively, in 29,867 mtDNA sequences (GenBank, February 2015). However, the affected positions show a low evolutionary conservation (23.5 %, 13.9 % and 14.1 % in 5,165, 5,177 and 4,925 eukaryote species, respectively, obtained from GenBank in February 2015) when compared with the conservation of

the p.MT-ATP6:L156 amino acid (99.0 % in 4,925 Eukaryota species) that causes MILS or NARP. The lack of evolutionary conservation suggests that these mutations would have little or no impact on phenotype. Therefore, we assume that the m.8993T>G transversion is responsible for the major phenotypic differences between mutant and wild-type cybrids that have the same nuclear background.

It has previously been reported that m.8993T>G mutant cybrids with the osteosarcoma 143B nuclear background showed reduced oxygen consumption (D'Aurelio et al. 2010; Lopez-Gallardo et al. 2014; Pallotti et al. 2004), decreased ATP levels (D'Aurelio et al. 2010; Fujita et al. 2007; Lopez-Gallardo et al. 2014; Pallotti et al. 2004; Sgarbi et al. 2009; Vazquez-Memije et al. 2009), diminished MIMP (Lopez-Gallardo et al. 2014), and increased reactive oxygen species (ROS) (Lopez-Gallardo et al. 2014; Wojewoda et al. 2010). Oxygen consumption was also reported to be reduced in m.8993T>G mutant cybrids with the cervical cancer HeLa EB8 nuclear background (Shidara et al. 2005). To confirm that the mutant cybrids used in the present study also showed reduced OXPHOS capability, we analyzed these mitochondrial variables. We found that oxygen consumption was significantly decreased in both Om and Am cybrids (see Supplemental Material, Figure S3A and Table S3). The ATP levels were significantly diminished in only the Om cybrid. In contrast with Om in which H_2O_2 was significantly higher than in Owti, H_2O_2 levels were decreased in Am cybrids compared with Awt, though not significantly so. It was previously reported that mitochondria of an m.8993T>G mutant osteosarcoma 143B cybrid generated MIMP at the same magnitude as the parental wild-type cells (Wojewoda et al. 2012). We found that, similar to Om cybrids (Lopez-Gallardo et al. 2014), the MIMP in Am cybrids was reduced (see Supplemental Material, Figure S3B), although the last result is based on visual assessment of a single sample.

These results confirm that the biochemical phenotypes of our cybrids are similar to other reported cybrids with the m.8993T>G mutation.

Effects of tributyltin chloride on cybrids

It was previously reported that mitochondrial respiration was significantly decreased in mice treated with TBTC (Ueno et al. 2003), and that oxygen consumption in human adipose tissue derived-stem cells (hASCs) was decreased in reponse to 100 nM TBTC (Llobet et al. 2015b). We found that TBTC ≥ 10 nM significantly decreased oxygen consumption in Om cybrids when compared with untreated cybrids (Figure 1A). TBTC ≥ 50 nM was required to significantly reduce oxygen consumption in Owt cybrids. There are negative and significant correlations between TBTC concentration and oxygen consumption in Owt (linear regression coefficient (β) for the change in $\%O_2$ consumption with a 1-nM increase in TBTC = –0.45; R^2 = 0.924; $P < 0.0001$) and Om (TBTC β = –0.41; $R^2 = 0.796$; $P < 0.0001$). For the majority of TBTC concentrations between 20 and 90 nM, the reduction in oxygen consumption in response to TBTC was significantly greater in Om than Owt cybrids.

Additionally, TBTC ≥ 20 nM significantly decreased oxygen consumption in Am cybrids when compared with untreated cybrids (Figure 1B). TBTC ≥ 70 nM significantly reduced oxygen consumption in Awt cybrids; however, 40 nM TBTC also reduced this parameter. There are negative and significant correlations between TBTC concentration and oxygen consumption in Awt (TBTC β = –0.35; $R^2 = 0.876$; $P < 0.0001$) and Am cybrids (TBTC β = –0.46; $R^2 = 0.956$; $P < 0.0001$). For TBTC concentrations between 30 and 90 nM, the reduction in oxygen consumption in response to TBTC was significantly greater in Am than Awt cybrids. The

decrease in oxygen consumption in response to 50 and 60 nM TBTC was significantly greater in Om than in Am cybrids, and the decrease in oxygen consumption in response to 90 and 100 nM TBTC was significantly greater in Owt than Awt cybrids.

Previous reports showed that 100 nM tributyltin decreased ATP levels in human embryonic carcinoma NT2/D1 cells (Yamada et al. 2014). We found that TBTC ≥ 15 nM significantly decreased ATP levels in Om and Am cybrids when compared with untreated cybrids (Figure 2). Furthermore, Owti and Awt cybrids treated with TBTC ≥ 60 nM and 90 nM, respectively, showed a significant reduction in ATP levels. These levels were also reduced in Owti cybrids treated with 15 nM TBTC. There are negative and significant correlations between TBTC concentrations and ATP levels in Owti (TBTC $\beta = -0.17$; $R^2 = 0.810$; $P = 0.0374$), Om (TBTC $\beta = -0.30$; $R^2 = 0.850$; $P = 0.0234$) and Am cybrids (TBTC $\beta = -0.38$; $R^2 = 0.780$; $P = 0.0491$) but not Awt cybrids (TBTC $\beta = -0.11$; $R^2 = 0.382$; $P = 0.3076$). Om and Am cybrids were more susceptible to TBTC concentrations ≥ 15 or ≥ 30 nM, respectively, when compared with the wild-type. The decrease in ATP levels in response to 90 nM TBTC was significantly greater in Am than Om cybrids. There was no significant difference in ATP levels between Owti and Awt cybrids at any dose.

In a previous study, MIMP was diminished in mouse thymocytes treated with 10 nM TBTC (Sharma and Kumar 2014). In the present study, visual assessment of a single sample suggests that TBTC ≥ 30 nM decreased the MIMP of the Am cybrid. However, a concentration ≥ 60 nM is required to affect the MIMP of the Awt cybrid (Figure 3).

In a preceding study, concentrations of TBTC 10 nM increased H_2O_2 production in mouse thymocytes (Sharma and Kumar 2014). However, in other studies, TBTC ≤ 300 nM did not increase H_2O_2 levels in dissociated mix cells from different parts of rat brain (Mitra et al. 2014),

and 100 nM TBTC did not change the H_2O_2 production in hASCs (Llobet et al. 2015b). We found that, TBTC ≥ 30 nM significantly decreased H_2O_2 production in Owti and Om cybrids when compared with untreated cybrids (Figure 4). There are negative and significant correlations between TBTC concentrations and H_2O_2 levels in Owti (TBTC $\beta = -0.56$; $R^2 = 0.969$; $P = 0.0006$) and Om cybrids (TBTC $\beta = -0.58$; $R^2 = 0.915$; $P = 0.0071$).

Tributyltin target

Several TBTC targets have been proposed. It has been reported that TBTC can activate genomic pathways by binding PPARγ (Kanayama et al. 2005). Thus, the different susceptibilities of mutant and wild-type cybrids to TBTC may be PPARγ-mediated. Osteosarcoma 143B and adenocarcinoma A549 cells express the PPARγ gene (Haydon et al. 2002; Li et al. 2014). However, we did not observe significant differences in PPARγ mRNA levels between mutant and wild-type cybrids (see Supplemental Material, Figure S3A). Therefore, this target does not explain our results.

A previous report showed that 100 nM TBTC decreased IDH activity in human embryonic carcinoma NT2/D1 cells. These results suggest that IDH is a novel target of TBTC (Yamada et al. 2014). IDH is a mitochondrial enzyme from the tricarboxylic acid cycle that produces NADH. This compound is reoxidized in the OXPHOS electron transport chain and increases oxygen consumption and MIMP and ATP production. Therefore, the inhibition of IDH by TBTC would decrease all of these parameters. However, we have previously found that 100 nM TBTC increased IDH activity in hASCs (Llobet et al. 2015b). To assess IDH inhibition, we tested the effect of TBTC on osteosarcoma 143B cybrids. At TBTC ≥ 20 nM, Owti IDH activity did not

differ significantly from untreated Owti cells. TBTC at 20 and 100 nM significantly increased IDH activity in the Om cybrid compared with untreated Om cells (Figure 5). These data suggest that NADH accumulated by OXPHOS dysfunction in mutant cybrids can provoke an abnormal increase in isocitrate and a compensatory expression of IDH. Indeed, the mutant cybrid showed significantly higher IDH activity than the Owti cybrid (see Supplemental Material, Figure S3A). Thus, inhibition of IDH does not explain our results.

CV is the third proposed target of TBTC. In previous studies it has been shown that, similar to TBTC, the CV inhibitor OLI ≥ 49 nM decreased oxygen consumption in osteosarcoma 143B cybrids (Gomez-Duran et al. 2010; McKenzie et al. 2007; Gomez-Duran et al. 2012; Zhang et al. 2012) and 3.15 μM OLI produced a decline in ATP production in these 143B cybrids (Gomez-Duran et al. 2010; McKenzie et al. 2007; Gomez-Duran et al. 2012). Furthermore, 3.15 μM OLI increased and 6 μM OLI decreased MIMP in osteosarcoma 143B cybrids (McKenzie et al. 2007; Porcelli et al. 2009). Surprisingly, in this study, a qualitative assessment suggests that MIMP was reduced in Awt cybrids in response to 16 nM OLI, but was reduced in Am cybrids in response to only 4 nM OLI (Figure 6A). OLI may cause a decrease in MIMP because there is not enough ATP to activate respiratory substrates (Brown et al. 1990). The effect of OLI on H_2O_2 levels also varies. Previous studies showed that 4 nM OLI increased these H_2O_2 levels in mouse preadipocytes 3T3-L1 (Carriere et al. 2003), and 16 nM OLI decreased H_2O_2 in hASCs (Llobet et al. 2015b). In both Om and Owt cybrids, 16 nM OLI decreased H_2O_2 levels (Figure 6B). Similar to hASCs (Llobet et al. 2015b), 16 nM OLI increased IDH activity in Om cybrids (Figure 6C). All of these results support CV as the target of TBTC (von Ballmoos et al. 2004). Further investigation to confirm the target of TBTC is required.

DISCUSSION

TBTC is a potent algicide and molluscicide that was used in marine antifouling ship paints (Grun 2014). Due to its adsorbing efficacy on sediments, long half-life and lipophilic nature, the levels of TBTC were considerably high in marine sediments and fishes (Mitra et al. 2014). Widespread environmental contamination of marine ecosystems with organotins began in the 1960s (Grun 2014). As a result, a global ban on the use of organotin-based antifouling paints was created in 2003 onward (Grun 2014). However, environmental contamination by organotins goes beyond aquatic ecosystems because they are also used in industrial and agricultural activities (Grun 2014). The slow rate of environmental degradation gives TBTC the potential for bioaccumulation in upper trophic species of the food chain. In fact, several studies have found TBT concentrations in human blood in the range of 8.3 - 293 nM (Kannan et al. 1999; Whalen et al. 1999). This range is consistent with the TBTC concentrations used in this study. However, tributyltin compounds may be metabolized to dibutyltin and other metabolites (Boyer 1989), and TBT is rapidly cleared from blood. Thus, blood would not be the ideal biological compartment for estimating butyltin burden in humans (Kannan et al, 1999). In liver samples from 9 Polish, 4 Japaneses and 18 Danish, ranges of 2.4 – 11; 59 – 96; y 1.1 – 33 ng of butyltin (TBT+DBT+MBT)/g of liver were found (Kannan et al. 1997; Nielsen et al. 2002; Takahashi et al. 1999).

Om and Owt cybrids (or Am and Awt cybrids) differ in their mtDNA genotype. The phenotypic differences provoked by TBTC between cybrids from the same nuclear genetic background suggest that mtDNA is the responsible factor. For the analysis of all mitochondrial variables, except oxygen consumption, in osteosarcoma 143B cybrids, we used isogenic cybrids

(Owti and Om). The Owti cybrid only differs from Om in the m.8993 nucleotide position. Our results suggest that this mtDNA nucleotide position is the factor responsible for the phenotypic differences in response to TBTC between these cells. Moreover, there is a higher similarity in the mitochondrial response to TBTC between the Om and Am cybrids (or between Owt/Owti and Awt cybrids), that harbor different nDNA and mtDNA but the same m.8993 nucleotide, than Om and Owt/Owti cybrids (or Am and Awt cybrids), that harbor the same nDNA or even the same mtDNA but differ in the m.8993 nucleotide. These results confirm that the m.8993T>G transversion is the responsible factor for the phenotypic differences between these cells in the response to TBTC. Therefore, a combination of this pathological mutation and this environmental contaminant could modify the phenotypic expression of the m.8993T>G mutation.

Several p.MT-ATP6 TMH4 and 5 amino acids from the CV proton channel are mutated in patients suffering from different mitochondriopathies (Lopez-Gallardo et al. 2014). The interaction of a particular mutation with an environmental factor, such as TBTC, may explain different pathological phenotypes. Interestingly, such an interaction might also explain why the m.9025G>A/p.MT-ATP6:G167S mutation, a candidate for the etiologic factor of a particular mitochondriopathy, is found in both patients and healthy individuals. The m.9025G>A mutation was found in a patient with loss of Purkinje cells (Lopez-Gallardo et al. 2014), and Purkinje cells showed degenerative changes throughout the tributyltin treated-rat cerebellum (Elsabbagh et al. 2002).

Organotin compounds are highly lipophilic and readily penetrate the blood-brain barrier to enter the brain (Kotake 2012). An *in vitro* study reported that a concentration of 30 nM TBTC caused a significant decrease in MIMP in dissociated mixed cells from different parts of the rat brain. Cells from the striatum showed a higher susceptibility than cells from other brain regions

(Mitra et al. 2014). Brain lesions, particularly in the striatum, characterize a group of disorders termed “striatal necrosis syndromes”. These disorders include familial bilateral striatal necrosis (FBSN), MILS and NARP, and they can be caused by *MT-ATP6* mutations (Schon et al. 2001). Interestingly, we found that levels of oxygen consumption, MIMP, and ATP production in wild-type cybrids following TBTC exposure were similar to levels in cybrids with *MT-ATP6* mutations before TBTC exposure. More experiments in primary cells, such as neurons, are required. However, our findings suggest that environmental-induced striatal necrosis syndromes due to xenobiotics, such as organotins, may be possible.

REFERENCES

Boyer IJ. 1989. Toxicity of dibutyltin, tributyltin and other organotin compounds to humans and to experimental animals. Toxicology 55(3): 253-298.

Brown GC, Lakin-Thomas PL, Brand MD. 1990. Control of respiration and oxidative phosphorylation in isolated rat liver cells. Eur J Biochem 192(2): 355-362.

Carelli V, Franceschini F, Venturi S, Barboni P, Savini G, Barbieri G, et al. 2007. Grand rounds: could occupational exposure to n-hexane and other solvents precipitate visual failure in leber hereditary optic neuropathy? Environ Health Perspect 115(1): 113-115.

Carriere A, Fernandez Y, Rigoulet M, Penicaud L, Casteilla L. 2003. Inhibition of preadipocyte proliferation by mitochondrial reactive oxygen species. FEBS Lett 550(1-3): 163-167.

Chomyn A, Lai ST, Shakeley R, Bresolin N, Scarlato G, Attardi G. 1994. Platelet-mediated transformation of mtDNA-less human cells: analysis of phenotypic variability among clones from normal individuals--and complementation behavior of the tRNALys mutation causing myoclonic epilepsy and ragged red fibers. Am J Hum Genet 54(6): 966-974.

Cooper DN, Krawczak M, Polychronakos C, Tyler-Smith C, Kehrer-Sawatzki H. 2013. Where genotype is not predictive of phenotype: towards an understanding of the molecular basis of reduced penetrance in human inherited disease. Hum Genet 132(10): 1077-1130.

D'Aurelio M, Vives-Bauza C, Davidson MM, Manfredi G. 2010. Mitochondrial DNA background modifies the bioenergetics of NARP/MILS ATP6 mutant cells. Hum Mol Genet 19(2): 374-386.

Degoul F, Diry M, Rodriguez D, Robain O, Francois D, Ponsot G, et al. 1995. Clinical, biochemical, and molecular analysis of a maternally inherited case of Leigh syndrome

(MILS) associated with the mtDNA T8993G point mutation. J Inherit Metab Dis 18(6): 682-688.

Elsabbagh HS, Moussa SZ, El-tawil OS. 2002. Neurotoxicologic sequelae of tributyltin intoxication in rats. Pharmacol Res 45(3): 201-206.

Enns GM, Bai RK, Beck AE, Wong LJ. 2006. Molecular-clinical correlations in a family with variable tissue mitochondrial DNA T8993G mutant load. Mol Genet Metab 88(4): 364-371.

Fujita Y, Ito M, Nozawa Y, Yoneda M, Oshida Y, Tanaka M. 2007. CHOP (C/EBP homologous protein) and ASNS (asparagine synthetase) induction in cybrid cells harboring MELAS and NARP mitochondrial DNA mutations. Mitochondrion 7(1-2): 80-88.

Gomez-Duran A, Pacheu-Grau D, Lopez-Gallardo E, Diez-Sanchez C, Montoya J, Lopez-Perez MJ, et al. 2010. Unmasking the causes of multifactorial disorders: OXPHOS differences between mitochondrial haplogroups. Hum Mol Genet 19(17): 3343-3353.

Gomez-Duran A, Pacheu-Grau D, Martinez-Romero I, Lopez-Gallardo E, Lopez-Perez MJ, Montoya J, et al. 2012. Oxidative phosphorylation differences between mitochondrial DNA haplogroups modify the risk of Leber's hereditary optic neuropathy. Biochim Biophys Acta 1822(8): 1216-1222.

Grun F. 2014. The obesogen tributyltin. Vitam Horm 94: 277-325.

Hao XD, Yang YL, Tang NL, Kong QP, Wu SF, Zhang YP. 2013. Mitochondrial DNA haplogroup Y is associated to Leigh syndrome in Chinese population. Gene 512(2): 460-463.

Haydon RC, Zhou L, Feng T, Breyer B, Cheng H, Jiang W, et al. 2002. Nuclear receptor agonists as potential differentiation therapy agents for human osteosarcoma. Clin Cancer Res 8(5): 1288-1294.

Holt IJ, Harding AE, Petty RK, Morgan-Hughes JA. 1990. A new mitochondrial disease associated with mitochondrial DNA heteroplasmy. Am J Hum Genet 46(3): 428-433.

Kanayama T, Kobayashi N, Mamiya S, Nakanishi T, Nishikawa J. 2005. Organotin compounds promote adipocyte differentiation as agonists of the peroxisome proliferator-activated receptor gamma/retinoid X receptor pathway. Mol Pharmacol 67(3): 766-774.

Kanan K, Falandysz J. 1997. Butyltin residues in sediment, fish, fish-eating birds, harbor porpoise and human tissues from the Polish coast of the Baltic Sea. Mar Pollut Bull 34(3): 203-207.

Kannan K, Senthilkumar K, Giesy JP. 1999. Occurrence of Butyltin Compounds in Human Blood. Environ Sci Technol 33(10): 1776-1779.

Kotake Y. 2012. Molecular mechanisms of environmental organotin toxicity in mammals. Biol Pharm Bull 35(11): 1876-1880.

Lake NJ, Bird MJ, Isohanni P, Paetau A. 2015. Leigh syndrome: neuropathology and pathogenesis. J Neuropathol Exp Neurol 74(6): 482-492.

Li J, Chen L, Yu P, Liu B, Zhu J, Yang Y. 2014. Telmisartan exerts anti-tumor effects by activating peroxisome proliferator-activated receptor-gamma in human lung adenocarcinoma A549 cells. Molecules 19(3): 2862-2876.

Llobet L, Montoya J, López-Gallardo E, Ruiz-Pesini E. 2015a. Side effects of culture media antibiotics on cell differentiation. Tissue Eng Part C Methods 21(11): 1143-1147.

Llobet L, Toivonen JM, Montoya J, Ruiz-Pesini E, López-Gallardo E. 2015b. Xenobiotics that affect oxidative phosphorylation alter differentiation of human adipose-derived stem cells at concentrations that are found in human blood. Dis Model Mech 8(11): 1441-1455.

Lopez-Gallardo E, Emperador S, Solano A, Llobet L, Martin-Navarro A, Lopez-Perez MJ, et al.

2014. Expanding the clinical phenotypes of MT-ATP6 mutations. Hum Mol Genet 23(23): 6191-6200.

McFarland R, Clark KM, Morris AA, Taylor RW, Macphail S, Lightowlers RN, et al. 2002. Multiple neonatal deaths due to a homoplasmic mitochondrial DNA mutation. Nat Genet 30(2): 145-146.

McKenzie M, Liolitsa D, Akinshina N, Campanella M, Sisodiya S, Hargreaves I, et al. 2007. Mitochondrial ND5 gene variation associated with encephalomyopathy and mitochondrial ATP consumption. J Biol Chem 282(51): 36845-36852.

Mitra S, Siddiqui WA, Khandelwal S. 2014. Early cellular responses against tributyltin chloride exposure in primary cultures derived from various brain regions. Environ Toxicol Pharmacol 37(3): 1048-1059.

Mkaouar-Rebai E, Chaari W, Younes S, Bousoffara R, Sfar MT, Fakhfakh F. 2009. Maternally inherited Leigh syndrome: T8993G mutation in a Tunisian family. Pediatr Neurol 40(6): 437-442.

Montoya J, Lopez-Gallardo E, Diez-Sanchez C, Lopez-Perez MJ, Ruiz-Pesini E. 2009. 20 years of human mtDNA pathologic point mutations: carefully reading the pathogenicity criteria. Biochim Biophys Acta 1787(5): 476-483.

Nielsen JB, Strand J. 2002. Butyltin compounds in human liver. Environ Res 88(2): 129-133.

Pallotti F, Baracca A, Hernandez-Rosa E, Walker WF, Solaini G, Lenaz G, et al. 2004. Biochemical analysis of respiratory function in cybrid cell lines harbouring mitochondrial DNA mutations. Biochem J 384(Pt 2): 287-293.

Porcelli AM, Angelin A, Ghelli A, Mariani E, Martinuzzi A, Carelli V, et al. 2009. Respiratory complex I dysfunction due to mitochondrial DNA mutations shifts the voltage threshold for

opening of the permeability transition pore toward resting levels. J Biol Chem 284(4): 2045-2052.

Prezant TR, Agapian JV, Bohlman MC, Bu X, Oztas S, Qiu WQ, et al. 1993. Mitochondrial ribosomal RNA mutation associated with both antibiotic-induced and non-syndromic deafness. Nat Genet 4(3): 289-294.

Rorbach J, Yusoff AA, Tuppen H, Abg-Kamaludin DP, Chrzanowska-Lightowlers ZM, Taylor RW, et al. 2008. Overexpression of human mitochondrial valyl tRNA synthetase can partially restore levels of cognate mt-tRNAVal carrying the pathogenic C25U mutation. Nucleic Acids Res 36(9): 3065-3074.

Ruhoy IS, Saneto RP. 2014. The genetics of Leigh syndrome and its implications for clinical practice and risk management. Appl Clin Genet 7: 221-234.

Schon EA, Santra S, Pallotti F, Girvin ME. 2001. Pathogenesis of primary defects in mitochondrial ATP synthesis. Semin Cell Dev Biol 12(6): 441-448.

Schwartzentruber J, Buhas D, Majewski J, Sasarman F, Papillon-Cavanagh S, Thiffault I, et al. 2014. Mutation in the nuclear-encoded mitochondrial isoleucyl-tRNA synthetase IARS2 in patients with cataracts, growth hormone deficiency with short stature, partial sensorineural deafness, and peripheral neuropathy or with Leigh syndrome. Hum Mutat 35(11): 1285-1289.

Sgarbi G, Casalena GA, Baracca A, Lenaz G, DiMauro S, Solaini G. 2009. Human NARP mitochondrial mutation metabolism corrected with alpha-ketoglutarate/aspartate: a potential new therapy. Arch Neurol 66(8): 951-957.

Sharma N, Kumar A. 2014. Mechanism of immunotoxicological effects of tributyltin chloride on murine thymocytes. Cell Biol Toxicol 30(2): 101-112.

Shidara Y, Yamagata K, Kanamori T, Nakano K, Kwong JQ, Manfredi G, et al. 2005. Positive contribution of pathogenic mutations in the mitochondrial genome to the promotion of cancer by prevention from apoptosis. Cancer Res 65(5): 1655-1663.

Takahashi S, Mukai H, Tanabe S, Sakayama K, Miyazaki T, Masuno H. 1999. Butyltin residues in livers of humans and wild terrestrial mammals and in plastic products. Environ Pollut 106(2): 213-218.

Tatuch Y, Christodoulou J, Feigenbaum A, Clarke JT, Wherret J, Smith C, et al. 1992. Heteroplasmic mtDNA mutation (T----G) at 8993 can cause Leigh disease when the percentage of abnormal mtDNA is high. Am J Hum Genet 50(4): 852-858.

Thorburn DR, Rahman S. 1993. Mitochondrial DNA-Associated Leigh Syndrome and NARP. In: Pagon RA, Adam MP, Ardinger HH, Wallace SE, Amemiya A, Bean LJH, Bird TD, Dolan CR, Fong CT, Smith RJH, Stephens K, editors. GeneReviews® [Internet]. Seattle (WA): University of Washington, Seattle; 1993-2015. 2003 Oct 30 [updated 2014 Apr 17].

Tsao CY, Mendell JR, Bartholomew D. 2001. High mitochondrial DNA T8993G mutation (<90%) without typical features of Leigh's and NARP syndromes. J Child Neurol 16(7): 533-535.

Ueno S, Kashimoto T, Susa N, Shiota Y, Okuda M, Mutoh K, et al. 2003. Effects of butyltin compounds on mitochondrial respiration and its relation to hepatotoxicity in mice and Guinea pigs. Toxicol Sci 75(1): 201-207.

van Oven M, Kayser M. 2009. Updated comprehensive phylogenetic tree of global human mitochondrial DNA variation. Hum Mutat 30(2): E386-E394.

Vazquez-Memije ME, Rizza T, Meschini MC, Nesti C, Santorelli FM, Carrozzo R. 2009. Cellular and functional analysis of four mutations located in the mitochondrial ATPase6

gene. J Cell Biochem 106(5): 878-886.

von Ballmoos C, Brunner J, Dimroth P. 2004. The ion channel of F-ATP synthase is the target of toxic organotin compounds. Proc Natl Acad Sci U S A 101(31): 11239-11244.

Whalen MM, Loganathan BG, Kannan K. 1999. Immunotoxicity of environmentally relevant concentrations of butyltins on human natural killer cells in vitro. Environ Res 81(2): 108-116.

Wojewoda M, Duszynski J, Szczepanowska J. 2010. Antioxidant defence systems and generation of reactive oxygen species in osteosarcoma cells with defective mitochondria: effect of selenium. Biochim Biophys Acta 1797(6-7): 890-896.

Wojewoda M, Duszynski J, Wieckowski M, Szczepanowska J. 2012. Effect of selenite on basic mitochondrial function in human osteosarcoma cells with chronic mitochondrial stress. Mitochondrion 12(1): 149-155.

Yamada S, Kotake Y, Demizu Y, Kurihara M, Sekino Y, Kanda Y. 2014. NAD-dependent isocitrate dehydrogenase as a novel target of tributyltin in human embryonic carcinoma cells. Sci Rep 4: 5952.

Zhang C, Huang VH, Simon M, Sharma LK, Fan W, Haas R, et al. 2012. Heteroplasmic mutations of the mitochondrial genome cause paradoxical effects on mitochondrial functions. FASEB J 26(12): 4914-4924.

FIGURE LEGENDS

Figure 1. Oxygen consumption by Osteosarcoma 143B (A) and Adenocarcinoma A549 (B) cybrids. The dashed line (100 %) represents the mean value in each of the untreated cybrids. The bars indicate the percentage of TBTC-treated cybrids. Error bars represent the standard deviation. * $P < 0.05$ vs. the same untreated cybrid; # $P < 0.05$ vs. the wild-type cybrid from the same nuclear background at the same TBTC concentration; † $P < 0.05$ for Om vs. Am or Owt vs. Awt at the same TBTC concentration.

Figure 2. ATP levels in Osteosarcoma 143B and Adenocarcinoma A549 cybrids. The dashed line (100 %) represents the mean value in each of the untreated cybrids. The bars indicate the percentage of TBTC-treated cybrids. Error bars represent the standard deviation. * $P < 0.05$ vs. the same untreated cybrid; # $P < 0.05$ vs. the wild-type cybrid from the same nuclear background at the same TBTC concentration; † $P < 0.05$ for Om vs. Am at the same TBTC concentration.

Figure 3. MIMP in single samples of TBTC-treated Adenocarcinoma A549 cybrids. A decreased red stain corresponds to a lower MIMP.

Figure 4. H_2O_2 production in TBTC-treated Osteosarcoma 143B cybrids. The dashed line (100 %) represents the mean value in each of the untreated cybrids. The bars indicate the percentage of treated cybrids. Error bars represent the standard deviation. * $P < 0.05$ vs. the same untreated cybrid.

Figure 5. IDH activity in TBTC-treated Osteosarcoma 143B cybrids. The dashed line (100 %) represents the mean value in each of the untreated osteosarcoma 143B cybrids. The bars indicate the percentage of treated cybrids. Error bars represent the standard deviation. * $P < 0.05$ vs. the same untreated cybrid. # $P < 0.05$ vs. the mutant cybrid treated with 20 nM TBTC.

Figure 6. Oligomycin (OLI) effect on different mitochondrial parameters. A) MIMP in single samples of treated Adenocarcinoma A549 cybrids. A decreased red stain corresponds to a lower MIMP. The uncoupler carbonyl cyanide m-chlorophenyl hydrazone (CCCP) was used as a control because it decreases MIMP. B) H_2O_2 production in treated Osteosarcoma 143B cybrids. C) IDH activity in treated Osteosarcoma 143B cybrids. The dashed line (100 %) represents the mean value in each of the untreated osteosarcoma 143B cybrids. The bars indicate the percentage of treated cybrids. Error bars represent the standard deviation. * $P < 0.05$ vs. the same untreated cybrid; # $P < 0.05$ vs. the wild-type cybrid at the same OLI concentration.

Figure 1

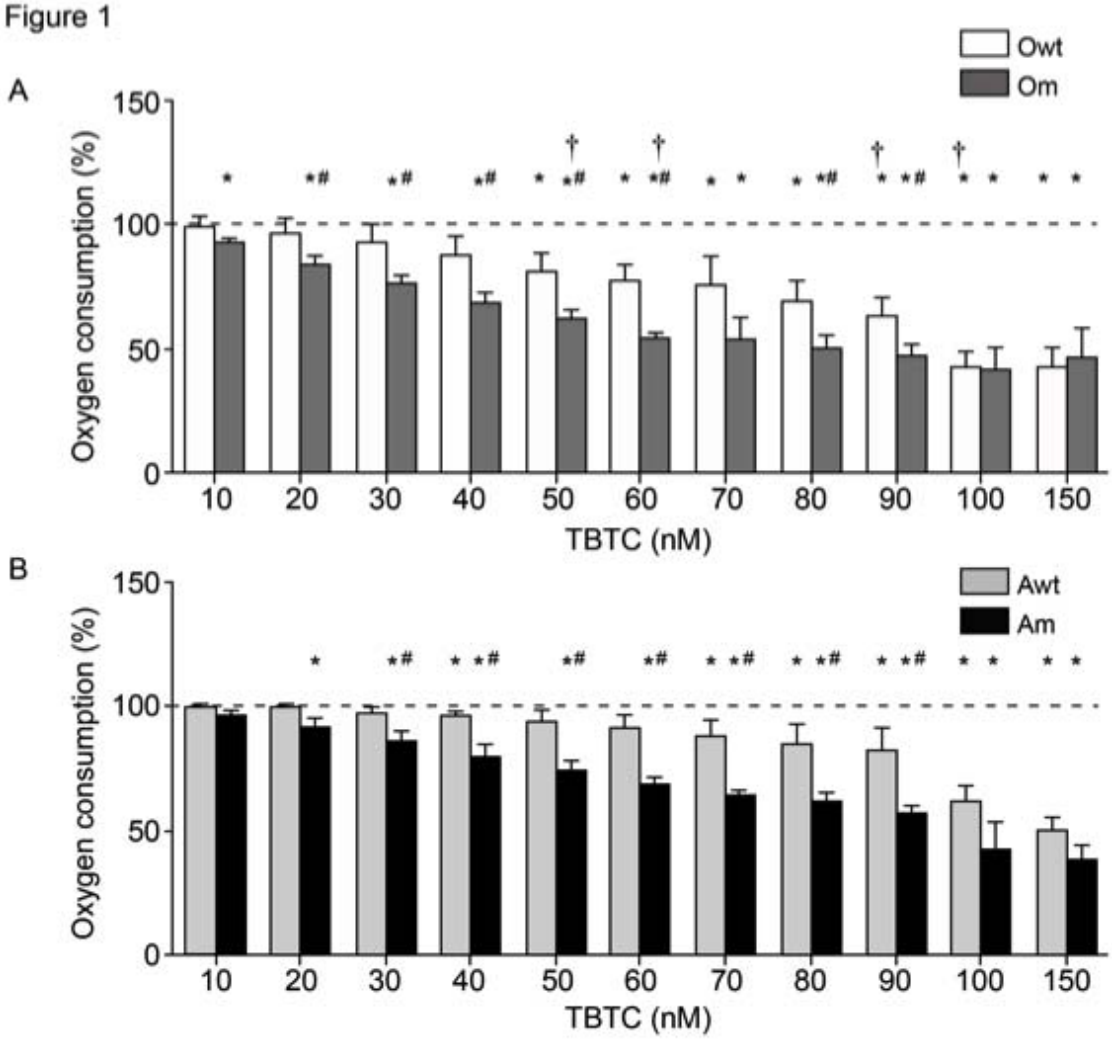
A
Owt
Om
Oxygen consumption (%)
150
100
50
0
10
20
30
40
50
60
70
80
90
100
150
TBTC (nM)
B
Awt
Am
Oxygen consumption (%)
150
100
50
0
10
20
30
40
50
60
70
80
90
100
150
TBTC (nM)

Figure 2

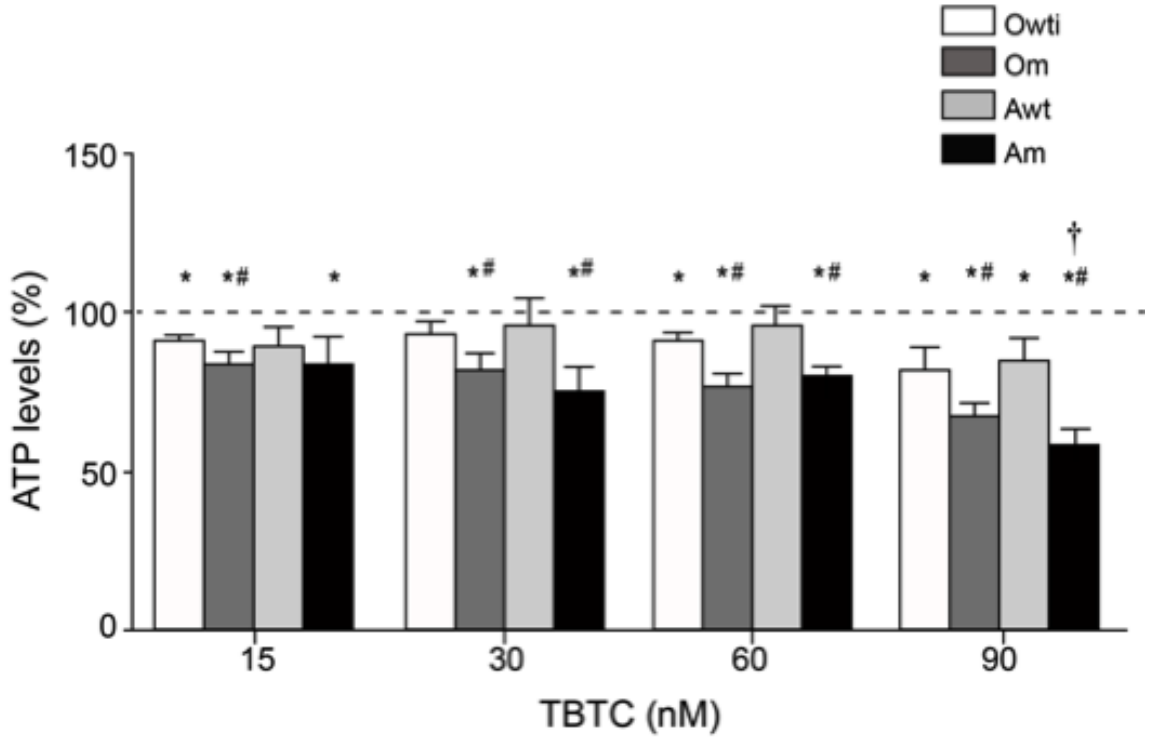

Figure 3

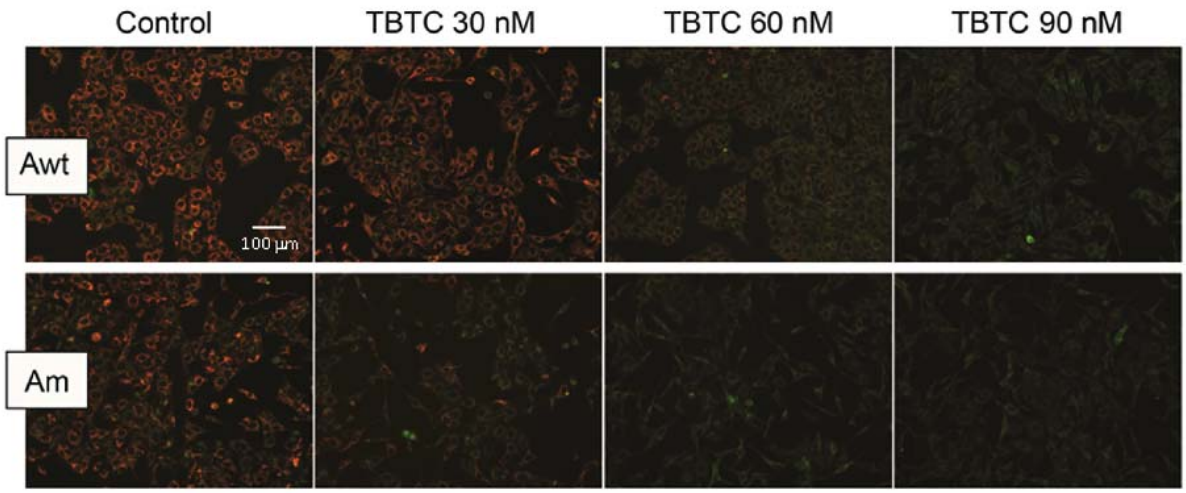

Figure 4

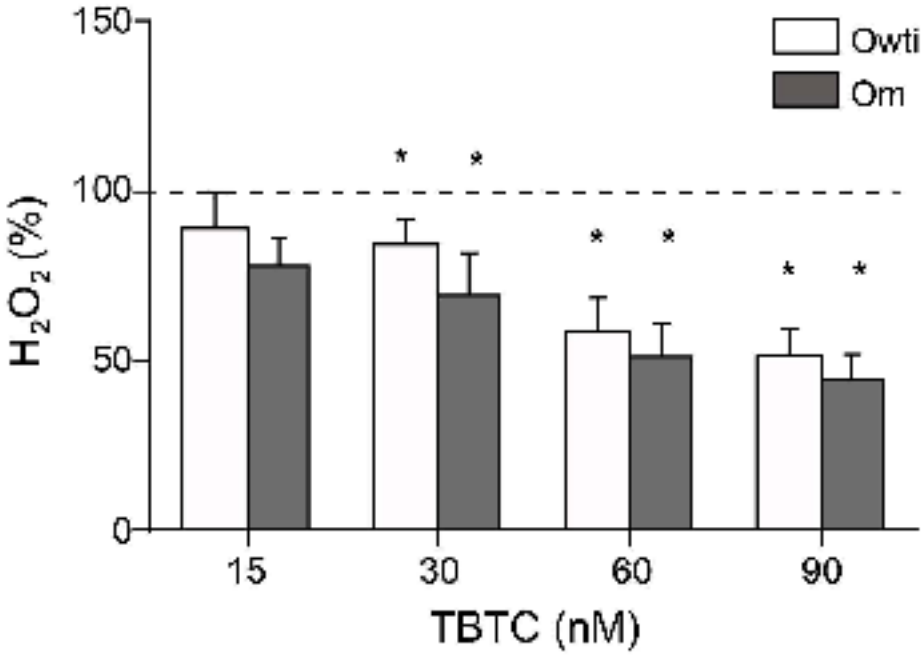

Figure 5

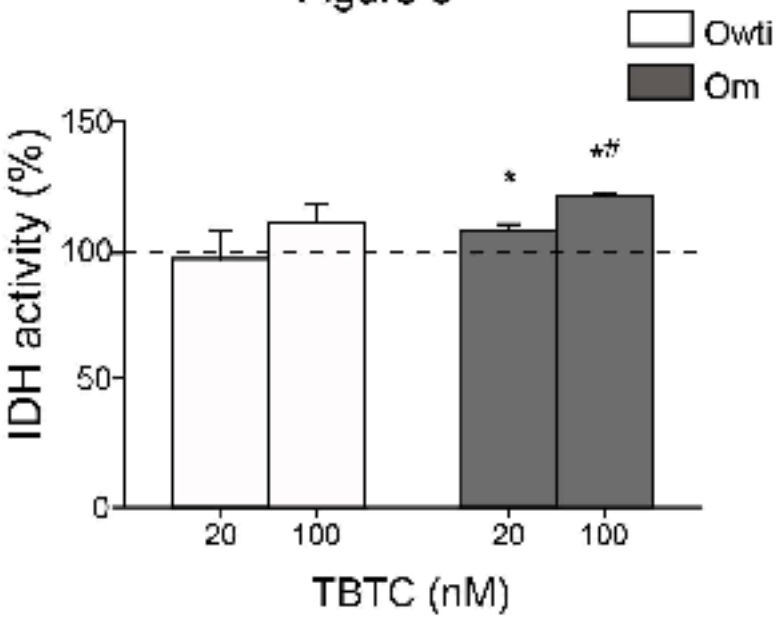

Figure 6

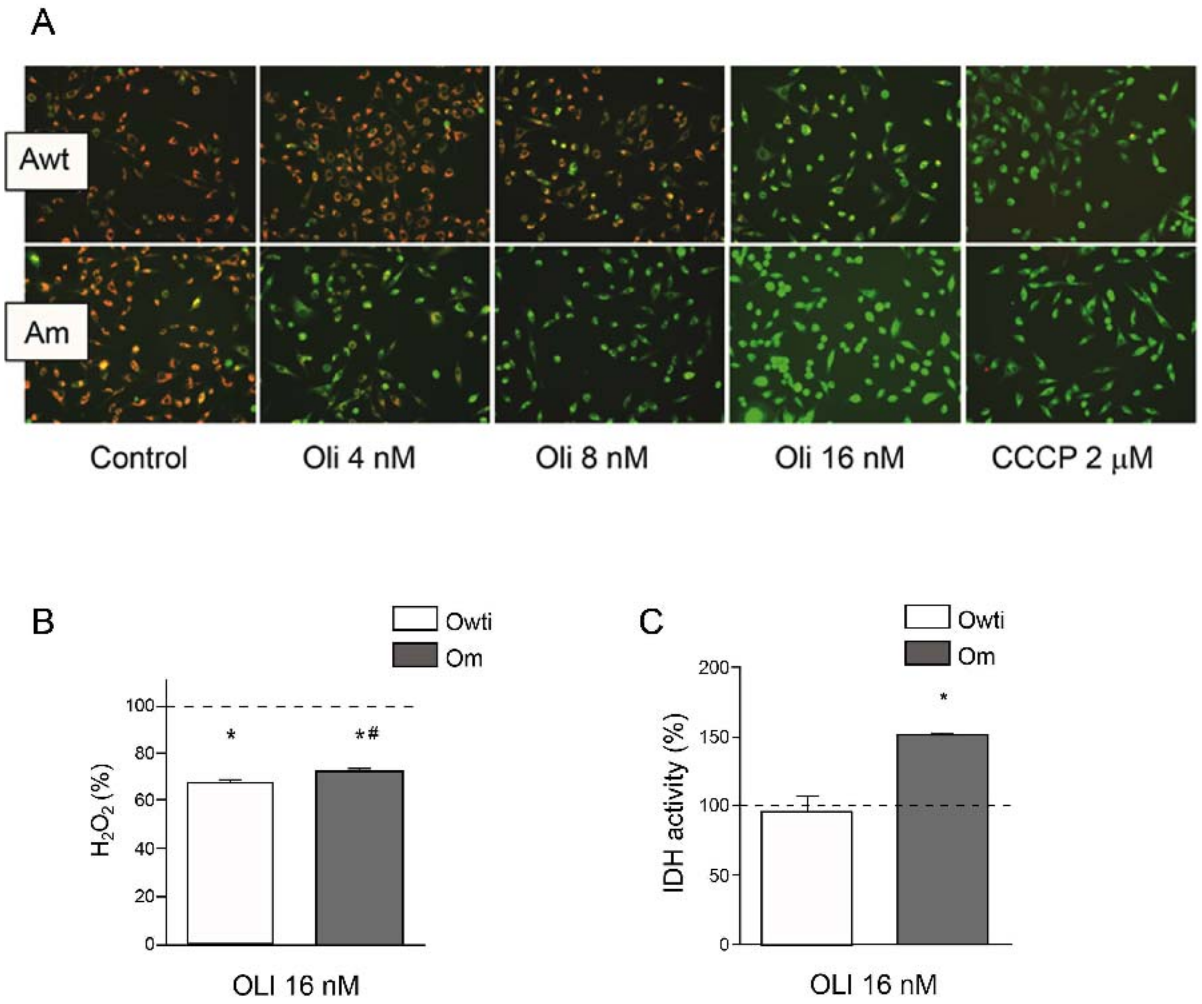
A
Awt
Am
Control
Oli 4 nM
Oli 8 nM
Oli 16 nM
CCCP 2 μM
B
Owti
Om
H_2O_2 (%)
100
80
60
40
20
0
*
*#
OLI 16 nM
C
Owti
Om
IDH activity (%)
200
150
100
50
0
*
OLI 16 nM